Vision Research 75 (2012) 60–70

Contents lists available at SciVerse ScienceDirect

Vision Research

journal homepage: www.elsevier.com/locate/visres

Fundus autofluorescence and optical coherence tomography in relation to visual function in Usher syndrome type 1 and 2

Ana Fakin [a,*], Martina Jarc-Vidmar [a], Damjan Glavač [b], Crystel Bonnet [c], Christine Petit [c,d,e], Marko Hawlina [a]

[a] Eye Hospital, University Medical Centre Ljubljana, Grablovičeva 46, 1000 Ljubljana, Slovenia
[b] Institute of Pathology, Medical Faculty, University of Ljubljana, Zaloška 4, 1000 Ljubljana, Slovenia
[c] Laboratory of Genetics and Physiology of Hearing, Inserm UMRS 587, Institut de la Vision, UPMC, 75012 Paris, France
[d] Institut Pasteur, 75015 Paris, France
[e] Collège de France, 75005 Paris, France

ARTICLE INFO

Article history:
Received 15 June 2012
Received in revised form 23 August 2012
Available online 18 September 2012

Keywords:
Usher syndrome
Retinitis pigmentosa
Fundus autofluorescence
Hyperautofluorescent ring
Foveal patch
Optical coherence tomography

ABSTRACT

Purpose of this study was to characterize retinal disease in Usher syndrome using fundus autofluorescence and optical coherence tomography. Study included 54 patients (26 male, 28 female) aged 7–70 years. There were 18 (33%) USH1 and 36 (67%) USH2 patients. 49/52 (94%) patients were found to carry at least one mutation in Usher genes. Ophthalmological examination included assessment of Snellen visual acuity, color vision with Ishihara tables, Goldmann visual fields (targets II/1–4 and V/4), microperimetry, fundus autofluorescence imaging and optical coherence tomography. Average age at disease onset (nyctalopia) was significantly lower in USH1 than USH2 patients (average 9 vs. 17 years, respectively; $p < 0.01$); however no significant differences were found regarding type of autofluorescence patterns, frequency of foveal lesions and CME, rate of disease progression and age at legal blindness. All representative eyes had abnormal fundus autofluorescence of either hyperautofluorescent ring (55%), hyperautofluorescent foveal patch (35%) or foveal atrophy (10%). Disease duration of more than 30 years was associated with a high incidence of abnormal central fundus autofluorescence (patch or atrophy) and visual acuity loss.

1. Introduction

Usher syndrome is a group of recessively inherited diseases, characterized by a combination of retinitis pigmentosa (RP) and sensorineural hearing loss. It has a prevalence of 3-6/100.000 (Millan et al., 2011) and represents 18% of all RP (Boughman, Vernon, & Shaver, 1983). Nine causative genes have been identified and three clinical types are known based on severity of hearing loss. Usher type 1 (USH1; *MYO7A*, *CDH23*, *PCDH15*, *USH1C* and *USH1G* genes) is characterized by severe congenital hearing loss while Usher type 2 (USH2; *USH2A*, *GPR98* and *DFNB31* genes) is characterized by moderate congenital hearing loss (Cohen, Bitner-Glindzicz, & Luxon, 2007). Usher type 3 (USH3; *USH3A* gene) is rare and characterized late onset progressive hearing loss (Saihan et al., 2009). Among all Usher genes, the three most commonly affected are *USH2A* (36–59%), *MYO7A* (10–18%) and *PCDH15* (4–6%) (Bonnet & El-Amraoui, 2011). Usher proteins were found to be integrated into a network in photoreceptor ciliary region, that could explain the common retinal phenotype (Lefevre et al., 2008; Maerker et al., 2008; Williams, 2008). Early histopathologic changes in RP are shortening of rod outer segments followed by rod cell death leading to nyctalopia (Milam, Li, & Fariss, 1998). With advancement, the retinal degeneration gives rise to a characteristic ring-shaped scotoma in the mid-periphery, which can expand to the periphery and macula. As the disease progresses, the cone photoreceptors also degenerate leading to loss of central vision (Milam, Li, & Fariss, 1998; van Soest et al., 1999). Fundus autofluorescence imaging (FAF) and optical coherence tomography (OCT) are used for morphological assessment of photoreceptors in the macular area (Mitamura et al., 2012). Various patterns of abnormal FAF have been reported in RP patients. Hyperautofluorescent ring can be seen in up to 60% of patients (Popovic, Jarc-Vidmar, & Hawlina, 2005; Robson et al., 2003) while central hyperautofluorescence was observed in 18% (Murakami et al., 2008). It is unclear whether any differences exist in retinal disease between different Usher types or genotypes. The most consistent

Abbreviations: FAF, fundus autofluorescence; OCT, optical coherence tomography; ISe, inner segment ellipsoid (also known as IS/OS junction); ELM, external (outer) limiting membrane; RP, retinitis pigmentosa; USH, Usher; VA, visual acuity; ISH, Ishihara color vision test; OPL, outer plexiform layer; IPL, inner plexiform layer; ONL, outer nuclear layer.

* Corresponding author. Address: Eye Hospital, University Medical Centre Ljubljana, Grablovičeva 46, 1000 Ljubljana, Slovenia. Fax: +386 1 522 1960.

E-mail addresses: ana.fakin@gmail.com (A. Fakin), damjan.glavac@mf.uni-lj.si (D. Glavač), crystel.bonnet@orange.fr (C. Bonnet), christine.petit@pasteur.fr (C. Petit), marko.hawlina@gmail.com (M. Hawlina).

0042-6989/$ - see front matter © 2012 Elsevier Ltd. All rights reserved.
http://dx.doi.org/10.1016/j.visres.2012.08.017

difference that is found is earlier onset of night blindness in USH1 than in USH2 (Tsilou et al., 2002). More severe form of retinitis pigmentosa in USH1 was reported by some authors (Edwards et al., 1998; Fishman et al., 1995; Hope et al., 1997; Piazza et al., 1986), however others did not share those findings (Kimberling et al., 1989; Seeliger et al., 1999; Tsilou et al., 2002).

The main aims of the study are to characterize the natural course of macular involvement in Usher syndrome using fundus autofluorescence and to compare FAF and OCT phenotypes associated with USH1 and USH2 genotypes.

2. Material and methods

2.1. Patients and study design

This prospective cross-sectional study included 54 patients with Usher syndrome (26 male, 28 female) aged from 7–70 years (average 44 ± 15). Six pairs of patients were siblings. Diagnosis of RP was based on nyctalopia, visual field constriction, pigmentary retinal changes, full-field scotopic and photopic electroretinography and genetic data where available. All patients had sensorineural hearing loss previously confirmed by audiometry. Ophthalmological examination included assessment of Snellen visual acuity (VA), color vision with Ishihara tables, Goldmann visual fields (targets II/1–4 and V/4), microperimetry, fundus autofluorescence imaging (FAF) and optical coherence tomography (OCT). Eyes with better quality of FAF and OCT images were chosen as representative eyes. Patients were asked about age when they first noticed night vision problems (nyctalopia). This age was used as disease onset in our study. Disease duration was calculated as time between onset of nyctalopia and examination date.

Molecular diagnosis was performed in 52 patients by sequencing of all exons and flanking intronic regions of nine known Usher genes. Statistical analysis was performed using PASW statistical software (PASW 18.0; PASW Inc., Chicago, IL). Study was approved by Slovenian Ethics Committee for Research in Medicine and all research procedures have been carried out in accordance with The Code of Ethics of the World Medical Association (Declaration of Helsinki) for experiments involving humans. Informed consent was obtained from all subjects.

2.2. Fundus autofluorescence and spectral-domain optical coherence tomography

Fundus autofluorescence imaging of 30° field of view and 8-mm Spectral-domain OCT scan through the fovea were performed simultaneously with a confocal scanning laser ophthalmoscope (OCT-SLO Spectralis, Heidelberg Engineering, Dossenheim, Germany) after pupil dilation with topical 1% Tropicamide. Patterns of FAF were determined in 51/54 patients. In three patients this was not possible due to imaging difficulties or severe cystoid macular edema (CME). Measurements of structures on FAF and OCT were performed using Spectralis software with micrometer caliper. Temporal horizontal radius of the hyperautofluorescent ring (distance from fovea to inner and outer border) or patch was measured on FAF image. Distance from the fovea along the horizontal midline to the location of disappearance of inner segment ellipsoid (ISe) junction and external limiting membrane (ELM) were measured on OCT. Thicknesses of the outer nuclear layer (from upper border of ELM/ONL to the upper border of OPL/INL) was measured in the fovea. Measurements of FAF structures, ELM and ISe were rounded to 0,01 mm to compensate for measurement error. Conversion of 1 mm of retina to 3.5° of visual field was used. Longitudinal changes in FAF were evaluated in 18 patients who have previously undertaken autofluorescence imaging. Visual function and retinal structure were compared between different FAF patterns in patients without media opacities or large CME ($N = 43$).

2.3. Microperimetry

Static microperimetry was performed with the Nidek MP1 (Nidek Technologies, Padua, Italy) after pupil dilation with topical 1% tropicamide. Minimum of 12 stimuli in the central 8° of retina were used. Stimuli of the size of Goldmann III target appeared for 200 ms and changed intensity in 4–2 strategy. Average retinal sensitivity of central 12 stimuli (8° of retina) was calculated using MP1 software. Additionally, kinetic microperimetry using 0 dB stimulus, size Goldmann III, moving in eight directions from 10° to the foveal center with velocity of 2.4°/s was performed on 10 patients with hyperautofluorescent rings.

3. Results

3.1. Clinical data

There were 18 (33%) USH1 patients with average age of 33 ± 16 years and 36 (67%) USH2 patients with average age of 49 ± 12 years. 49/52 (94%) analyzed patients were found to carry at least one mutation in Usher genes. Among those, there were

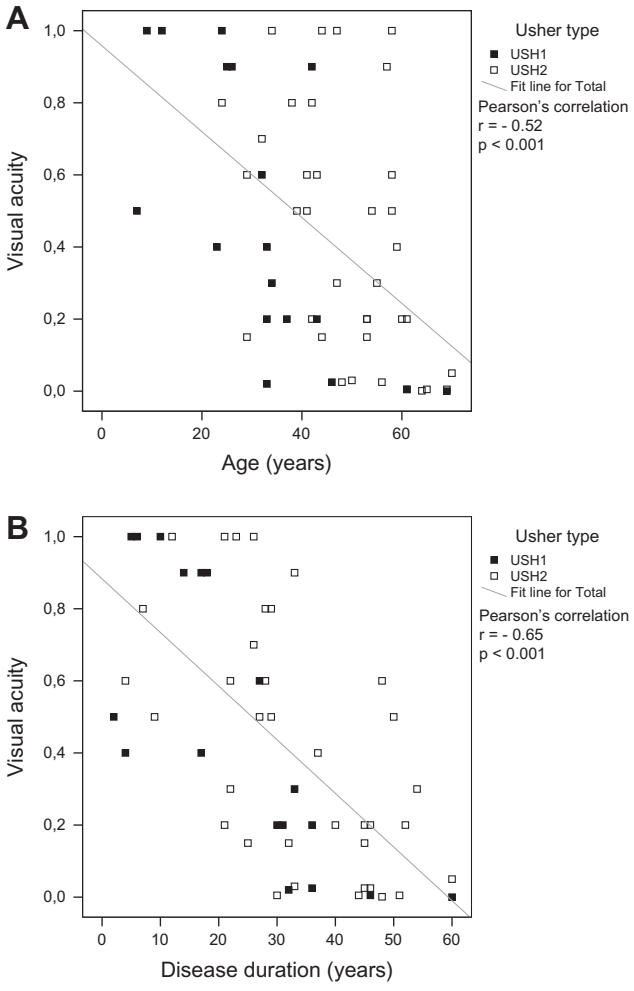

Fig. 1. Visual acuity in association with age (A) or disease duration (B) in Usher patients ($N = 43$). Patients with media opacities or large CME were excluded. Correlation was stronger between visual acuity and disease duration ($r = -0.65$) than between visual acuity and age ($r = -0.52$). It was significant in both cases ($p < 0.001$, Pearson's correlation).

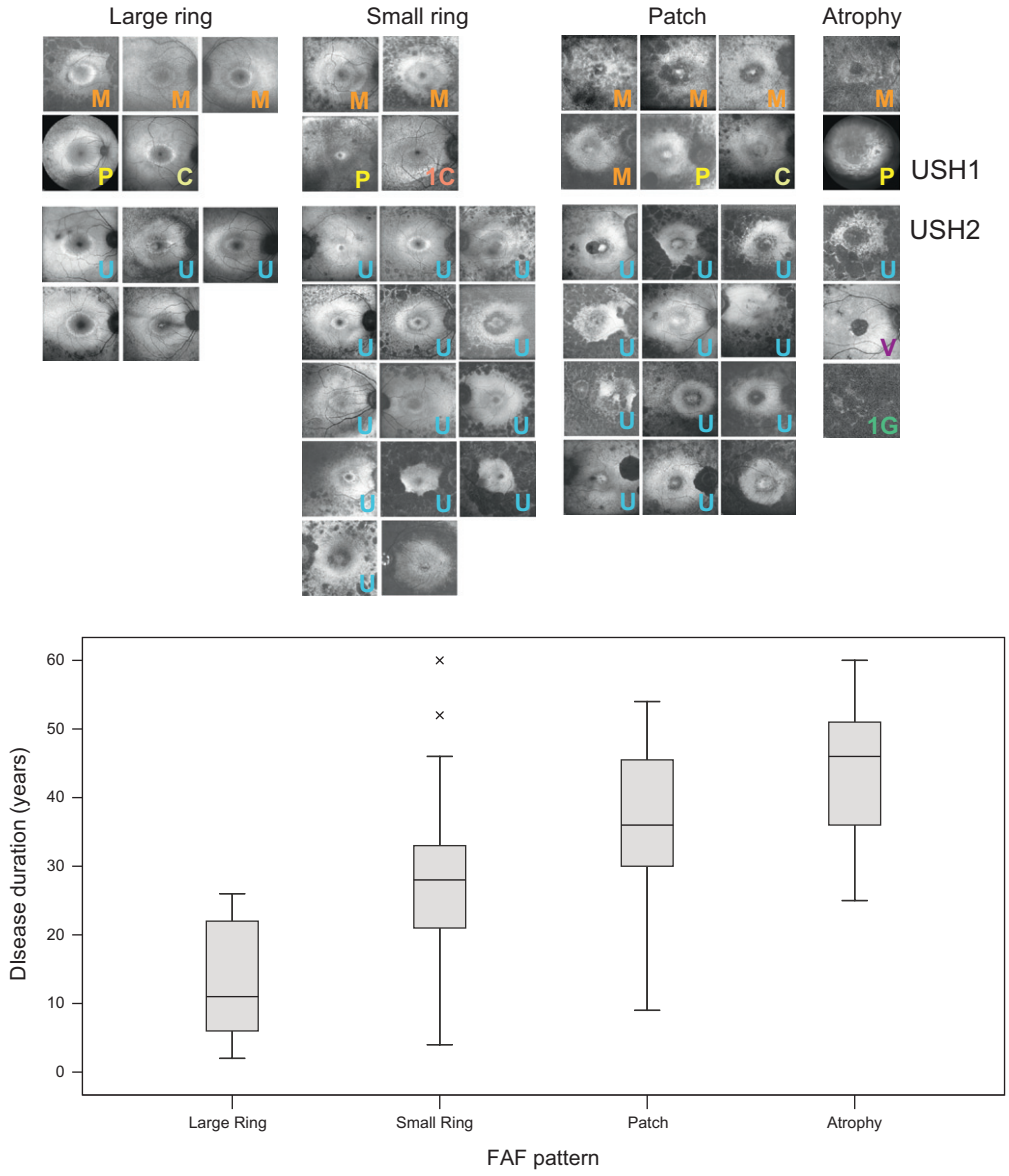

Fig. 2. Fundus autofluorescence of 51 patients with different types of Usher syndrome. Eyes with better image quality are presented. Three patients were excluded due to large CME or imaging difficulties. FAF patterns were divided into categories of large ring (radius ⩾ 3°), small ring (radius < 3°), foveal patch and atrophy. Genotyped patients are marked with capital letters (M = *MYO7A*, P = *PCDH15*, C = *CDH23*, 1C = *USH1C*, U = *USH2A*, V = *VLGR1*, 1G = *USH1G*). Below is a box plot graph showing disease duration in different FAF categories.

Table 1
Frequency of FAF patterns of ring, patch and atrophy in Usher patients with known genotypes. All three patterns were observed in the three most commonly affected genes (*USH2A*, *MYO7A* and *PCDH15*). In one USH2A patient and one MYO7A patient pattern was unable to be determined due to cystoid macular edema and imaging difficulties, respectively. FAF = fundus autofluorescence.

USH type	USH2	USH1					
Genotype	USH2A	MYO7A	PCDH15	CDH23	VLGR1	USH1C	USH1G
N	29	11	4	2	1	1	1
Avg. age (years)	50	33	40	20	29	23	48
Avg. age at onset (years)	17	9	10	4	4	19	2
Avg. disease duration (years)	33	24	30	17	25	4	46
FAF pattern frequency							
Ring (percent, *N*)	48% (14)	46% (5)	50% (2)	50% (1)		100% (1)	
Patch (percent, *N*)	31% (9)	36% (4)	25% (1)	50% (1)			
Atrophy (percent, *N*)	3% (1)	9% (1)	25% (1)		100% (1)		100% (1)
Ring on one eye and patch on the other	10% (3)						
Patch on one eye and atrophy on the other	4% (1)						

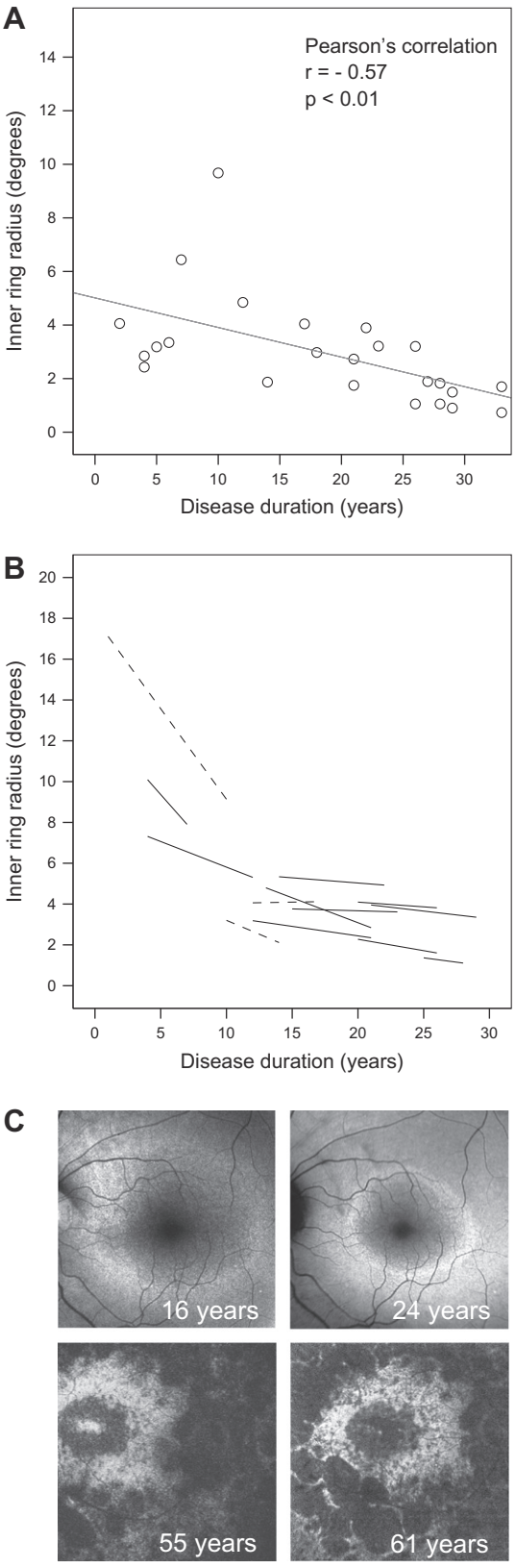

Fig. 3. (A) Inner ring radius in association with disease duration ($N = 24$). Four patients were excluded because of difficulties in FAF analysis due to CME (3) or cataract (1). (B) Spaghetti graph showing decrease of inner ring radius over the years in 13 patients with Usher syndrome. Dashed lines represent USH 1 patients. (C) Sequential fundus autofluorescence imaging of two patients showing ring constriction (up) and progression from patch to atrophy (bottom). Age at the time of examination is marked on FAF images.

59% (29) *USH2A*, 22% (11) *MYO7A*, 8% (4) *PCDH15*, 4% (2) *CDH23*, 2% (1) *VLGR1*, 2% (1) *USH1C* and 2% (1) *USH1G* patients. Average age at disease onset (nyctalopia) was 14 years (range 1–39) and was significantly lower in USH1 patients (average 9 years) than USH2 patients (average 17 years), $p < 0.01$. Average disease duration was 30 years (range 2–60 years). VA on the better eye ranged from 1.0 (20/20) to light perception. Correlation between visual acuity and disease duration was stronger than correlation between visual acuity and age. It was significant in both cases (Fig. 1). VA less than <0.05 (20/400) on the better eye, classified as blindness by World Health Organization, was found in 9/54 (17%) patients (3 USH1, 6 USH2). They were 60 ± 8 years old with 45 ± 9 years of disease duration. Age and disease duration of those patients was not significantly different between USH1 and USH2 patients. There were three children with Usher type 1, ages 7, 9 and 12 years. All three children had a hyperautofluorescent ring and CME at the time of presentation.

3.2. Fundus autofluorescence patterns

All patients had abnormal fundus autofluorescence. Three main patterns were recognized, namely hyperautofluorescent ring, hyperautofluorescent foveal patch and abnormal central hypoautofluorescence (atrophy). Ring was further divided into two subcategories (large and small) in respect to radius of inner ring border (Fig. 2). All FAF patterns could be seen in USH1 and USH2 patients and also in patients with the three most commonly affected genes (*USH2A*, *MYO7A* and *PCDH15*) (Table 1 and Fig. 2). Asymmetric FAF was observed in 5/51 (10%) patients. One *USH1C* patient had rings with large difference in size, three USH2A patients had a combination of unilateral ring and unilateral patch (two are shown in Fig. 4E) and one *USH2A* patient had a combination of unilateral patch and unilateral central hypoautofluorescence.

3.2.1. Hyperautofluorescent ring

Hyperautofluorescent ring was seen in 28/51 (55%) representative eyes. 22/28 (79%) of rings were surrounded with a ring of decreased autofluorescence (Fig. 2) which in some cases correlated with RPE atrophy on OCT. All rings were located inside vascular arcades. Location of inner and outer ring border could be determined in 24/28 patients; in four patients this was not possible due to cataract and/or CME. Internal radii ranged from 0.21 to 2.77 mm and external radii from 0.52 to 3.32 mm. Average ring width was 0.56 ± 0.32 mm. Inner ring radius was smaller in patients with longer disease duration (Fig. 3A). Average visual acuity in patients without media opacities or CME ($N = 20$) was 0.8 ± 0.2 (range, 0.3–1.0).

3.2.2. Hyperautofluorescent foveal patch

Hyperautofluorescent foveal patch was seen in 18/51 (35%) eyes. It was surrounded by a ring of decreased or absent autofluorescence (Fig. 2) which in 17/18 patients correlated with RPE atrophy on OCT (examples in Fig. 6, third and fourth column). Presence of patch was associated with longer disease duration (average 37 years) than presence of ring (average 23 years) (t-test, $p = 0.001$). Radius of patch ranged from 0.22 to 0.86 mm (average 0.52 mm) and did not correlate with disease duration (Pearson's correlation, $r = 0.16$, $p = 0.56$). Average visual acuity in patients without media opacities or CME was 0.2 ± 0.2 (range, 0.001–0.6).

3.2.3. Central hypoautofluorescence (atrophy)

Abnormal foveal hypoautofluorescence (atrophy) was seen in 5/51 (10%) eyes. It was surrounded with variable amount of residual perifoveal autofluorescence (Fig. 2). VA ranged from 0.15 to no light perception (average 0.04 ± 0.06).

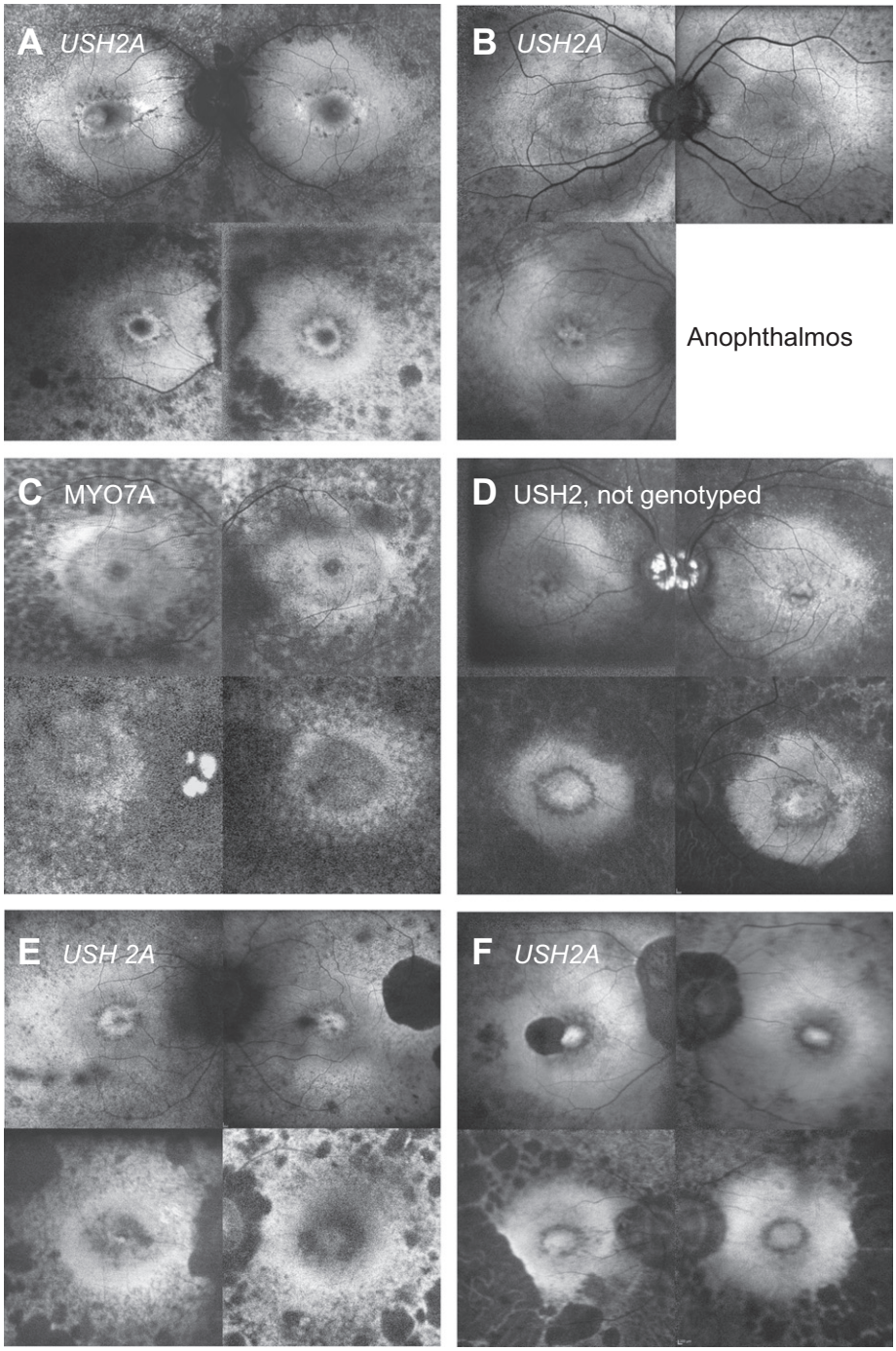

Fig. 4. Fundus autofluorescence in six pairs of siblings (A–F) with Usher syndrome. Specific details appeared similar between siblings, such as small dark spots on the outer ring border (A), large spots of atrophy (E and F) and peripapillary atrophy (F). Autofluorescence pattern on the periphery was also similar in all pairs. Differences between siblings included presence of cystoid macular edema (B bottom and D up) and optic disc drusen (D up and C bottom). Bottom sibling in pair B has had left eye enucleated due to neovascular glaucoma.

3.3. Fundus autofluorescence in siblings with Usher syndrome

Six pairs of siblings with Usher syndrome were included in this study (Fig. 4). Because siblings have presumably the same mutations (confirmed in five pairs), we analyzed their FAF patterns for genotype specific characteristics. Four pairs presented with matching patterns, including bilateral ring (Fig. 4A and B), bilateral patch (Fig. 4F) or combination of unilateral ring and unilateral patch (Fig. 4E). Two pairs presented with different FAF patterns (Fig. 4C and D), possibly as a result of different disease duration (pair C 14 and 27 years, pair D 46 and 54 years). Common characteristics included similar pattern of peripheral autofluorescence, small dark spots on the outer ring border, large spots of atrophy and/or peripapillary atrophy. Differences that were observed between siblings included presence of cystoid macular edema and optic disc drusen (Fig. 4).

3.4. Visual field in relation to fundus autofluorescence

Residual visual field (tested with Goldmann V/5 target) was detected in average of 7° eccentrically to the outer ring or patch border. Goldmann II/4 target was detected eccentrically to the outer ring/patch border in all patients with large rings, 83% of patients

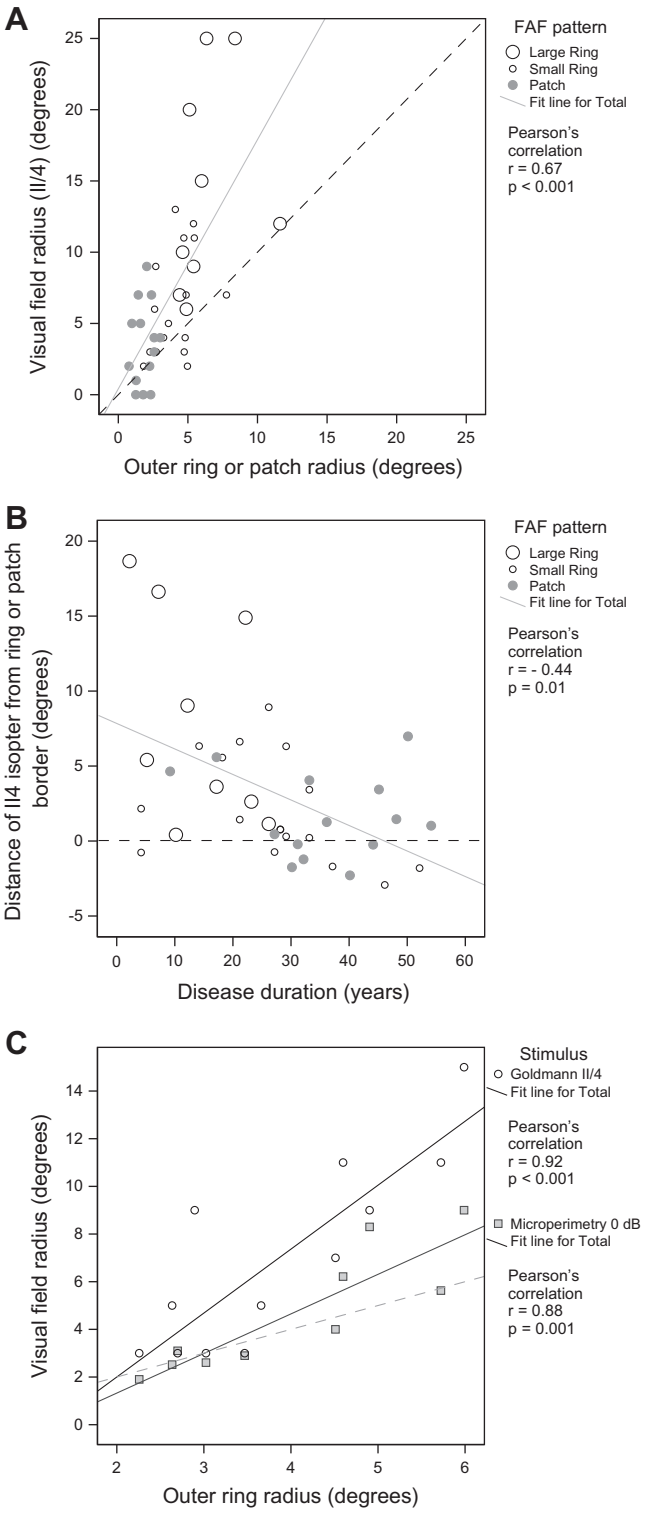

Fig. 5. Visual field in relation to fundus autofluorescence. (A) In majority of patients, visual field measured with Goldmann II/4 stimulus distended over larger area than the ring or patch on FAF. (B) Eccentricity of visual field from outer ring/patch border in association with disease duration. Border of preserved visual field was closer to the ring/patch in patients with long-standing disease. (C) Comparison of microperimetry and Goldmann perimetry in relation to ring radius. Goldmann II/4 target was usually detected further away than the highest intensity stimulus (0 dB) on microperimetry. Dashed line represents a situation where testing stimulus is detected exactly on the outer border of ring/patch (radius of visual field equals radius of autofluorescence).

with small rings and 64% of patients with patches (in average 7°, 3° and 2° eccentrically to border of hyperautofluorescence) (Fig. 5A). Eccentricity of II/4 visual field in relation to AF border decreased with disease duration (Pearson's correlation, $r = -0.4$, $p = 0.01$) (Fig. 5B). Goldmann II/1 target was detected by all patients with large rings and 58% of patients with small rings, in average 1° internally to the inner ring border. Ten patients with hyperautofluorescent rings additionally underwent kinetic microperimetry with stimulus of highest intensity (0 dB). In those patients temporal radii of visual fields measured by Goldmann perimetry (II/4 and II/3) and microperimetry were compared. Goldmann visual field using II/4 stimulus was in average 2.4 ± 2.3° larger than MP visual field (Fig. 5C). Goldmann visual field using II/3 stimulus was in average 0.4 ± 1.3° smaller than MP visual field.

3.5. Optical coherence tomography findings

In all eyes with rings, OCT revealed preserved ELM and ISe across the fovea. In eyes with patch, foveal ELM was seen in all cases and remains of ISe were found in 5/18 (28%) cases (average radius 0.21 mm). Eyes with patches that had remains of ISe had significantly better VA than eyes without it (average 0.5 vs. 0.1; $p < 0.001$). Foveal ONL thickness was not significantly different between the two groups (average 55 vs. 56 μm; $p = 0.9$). In eyes with central hypoautofluorescence, OCT revealed severely disorganized retinal structure with areas of RPE atrophy. Neither ISe nor ELM could be recognized (Fig 6, last column). In eyes with preserved ISe (all eyes with ring and 5/18 eyes with patch), visual acuity and color vision were low when ISe loss encroached on fovea (radius 500 μm), regardless of FAF pattern of ring or patch (Fig. 7).

3.5.1. Correlations between structures on FAF and OCT

In aligned photos of FAF and OCT we observed spatial correlations between inner/outer ring borders and ISe/ELM disruption. Inner ring border was located at approximately the same location as ISe disruption and outer ring border was located are approximately the same location as ELM disruption (point where ELM disappeared or fused with RPE) (Fig. 8). We were interested whether the correlations were exact; therefore we calculated average distances between corresponding structures on FAF and OCT. In average, distance between inner ring border and ISe disruption was 0.13 ± 0.21 mm (range, −0.01 to 0.65 mm; inner ring border was closer to the fovea). Out of the four cases with the largest difference (>0.30 mm), one had large CME (Fig. 8D), one had microcysts and two were without CME. Average difference between outer ring border and ELM disruption was 0.01 ± 0.16 mm (range, −0.44 to 0.29 mm; outer ring border was located closer to the fovea than ELM loss). In eyes with patch, there was a spatial correlation between patch border and horizontal span of ELM (Fig. 6, third and fourth column; Fig. 8B). In average, ELM loss appeared 0.04 mm closer to the fovea than patch border.

3.5.2. Cystoid macular edema

Cystic changes on OCT were seen in at least one eye of 56% (30/54) of patients. They were present in 56% (10/18) of USH1 and 56% (20/36) of USH2 patients. Out of patients with CME, 23% (7/30) had large CME, 57% (17/30) mild CME and 20% (6/30) had micro cystic changes on the more affected eye. Cysts were present in INL (60%, 18), INL and ONL (33%, 10) or OPL (7%, 2). Location or frequency of CME was not dependent on USH type.

3.6. Progression of disease in Usher syndrome

Disease progression in the retina was studied with longitudinal and cross-sectional analysis. Visual function and retinal structure were strongly associated with disease duration (Fig. 9).

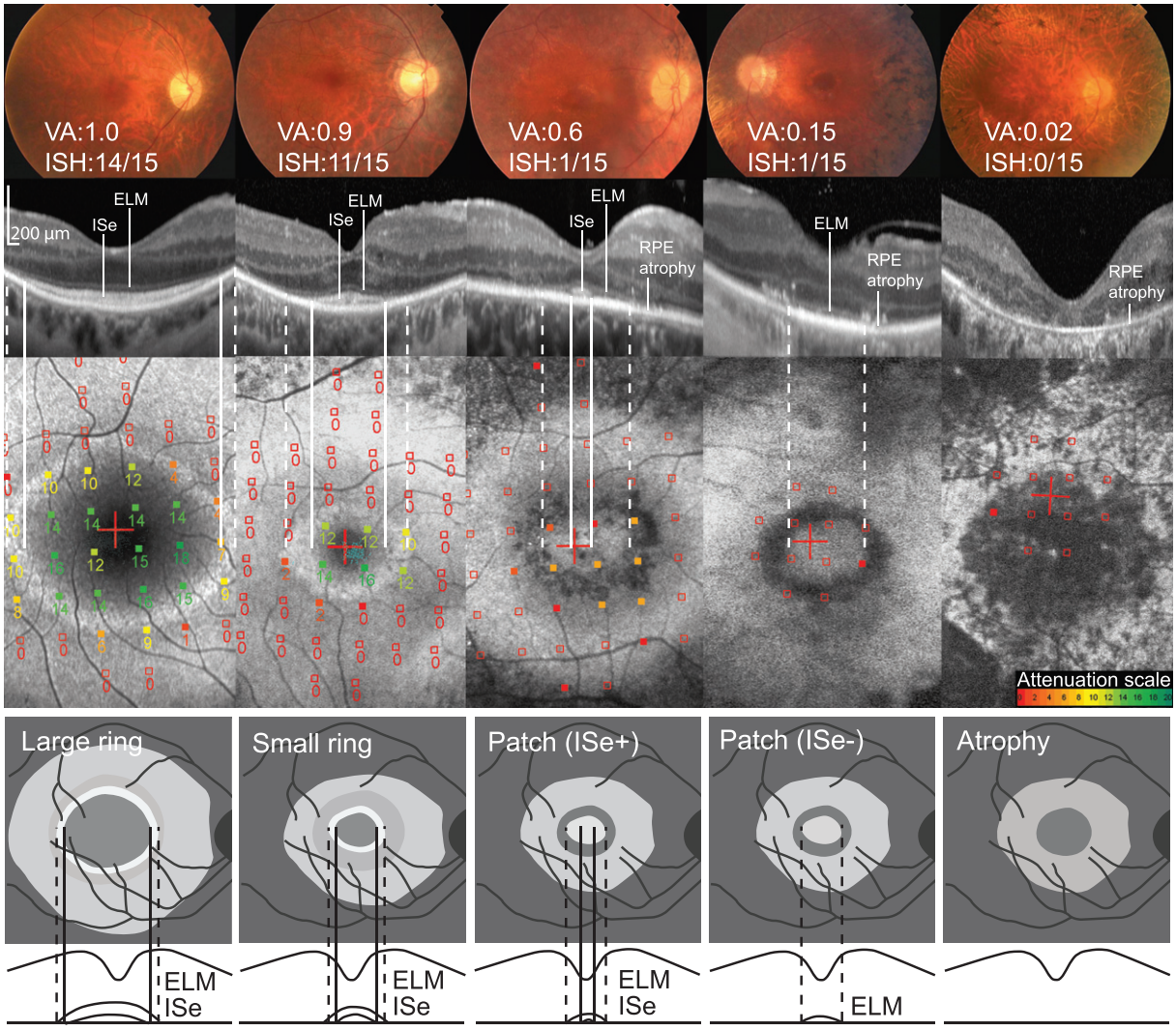

Fig. 6. Examples of Usher patients with different FAF patterns. Fundus photographs, optical coherence tomography and autofluorescence overlaid with microperimetry are shown. White lines show the point of ISe loss and dashed white lines show point of ELM loss. Below is a schematic representation of proposed disease progression. FAF = fundus autofluorescence, ISe = inner segment ellipsoid, ELM = external limiting membrane.

3.6.1. Longitudinal analysis of fundus autofluorescence

Longitudinal changes were assessed in 18 patients who have previously undergone FAF imaging.

Thirteen patients (3 USH1, 10 USH2, without large CME) at baseline imaging presented with hyperautofluorescent ring with average radius of 1.55 ± 1.19 mm. At follow up (7 ± 2 years), ring was seen again in all patients with average inner ring radius of 1.15 ± 0.67 mm. None of the patients developed central patch or hypoautofluorescence. Ring constriction was observed in 12/13 patients (Fig. 3B). Average rate of ring inner border constriction was 0.06 mm (range, 0.00–0.25 mm) or 4% (range, 0–9%) of starting radius per year. Outer ring border could be detected in 12/13 patients. Its average rate of constriction was 0.06 mm (0.00–0.23 mm) or 3% (range, 0–10%) per year. Rate of constriction was not dependent on USH type. After excluding two patients with changes in media opacities and one for lack of visual acuity data, there was a significant drop in average visual acuity in this group (from 0.94 to 0.88, $p < 0.01$). Out of those patients, four were without CME, three had microcysts and three had mild CME.

Five patients at baseline imaging presented with foveal patch. In two of them patch remained at follow-up after 5 years with change in radius from 0.65 to 0.60 and 0.74 to 0.70 mm, respectively. Average rate of patch radius constriction was 0.01 mm or 1% per year. Visual acuity in those patients remained unchanged and was 0.6 in patient with central remains of ISe and 0.015 in patient with absent ISe. In three patients patch was replaced with central hypoautofluorescence (atrophy) at follow-up after 6–9 years (Example in Fig. 3C). Average VA in those patients decreased from 0.28 to 0.08.

3.6.2. Cross-sectional analysis of fundus autofluorescence

FAF images were organized into categories of large ring ($\geqslant 3°$ internal radius), small ring (<3° internal radius), patch and central hypoautofluorescence (atrophy) and average disease duration was calculated for different categories. Ring was observed mainly in patients with up to 30 years of disease (large ring average 13 years, range 2–26; small ring average 28 years, range 4–60) whereas patch and atrophy were observed in patients with longer disease duration (patch average 36 years, range 9–54; atrophy average 44 years, range 25–60) (Fig. 2). Difference in disease duration was significant between patients with small ring and patch and not significant between large and small ring or patch and atrophy (Table 2). Retinal structure (ONL thickness, ELM radius, ISe radius) and function (VA, color vision, visual field, retinal sensitivity) decreased significantly in association with FAF changes (Pearson's correlation, $p < 0.001$ for all) (Table 2, examples in Fig. 6). Foveal

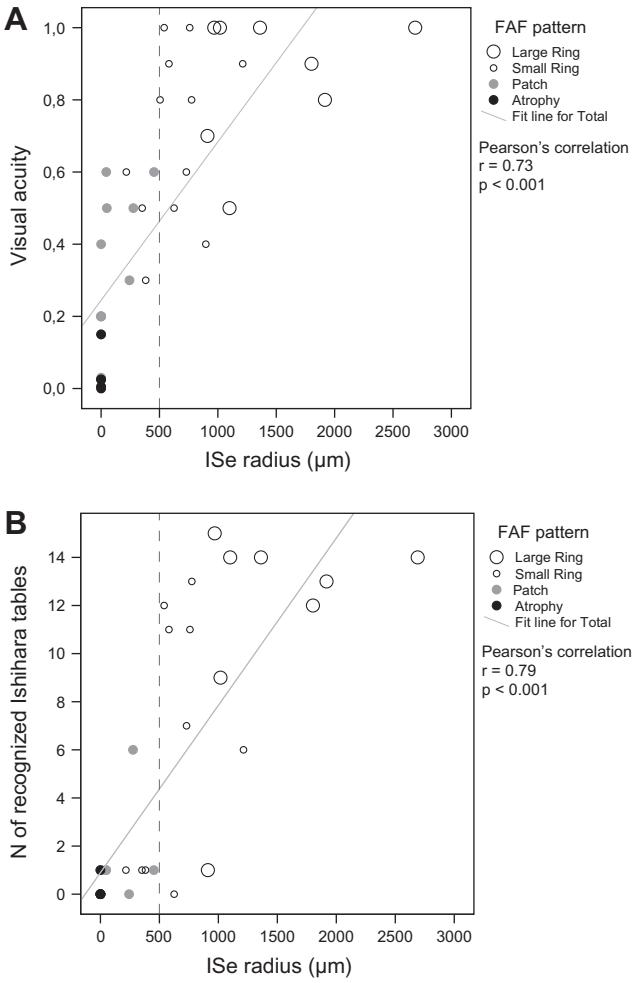

Fig. 7. Visual acuity (A) and color vision (B) in relation to ISe radius. Short ISe radius (<500 μm) was associated with low visual acuity and color vision, regardless of FAF pattern.

lesion (patch or atrophy) in one or both eyes was observed in 3/11 (27%) of USH1 and 4/17 (24%) of USH2 patients with up to 30 years of disease and in 5/6 (83%) of USH1 and 13/17 (76%) of USH2 patients with more than 30 years of disease. Frequencies were not significantly different between USH1 and USH2 patients (Fisher's exact test, $p > 0.5$).

4. Discussion

This study suggests that Usher syndrome patients have common morphological stages of retinal disease in the macula that can be characterized by FAF patterns of ring, patch and foveal atrophy. Ring represents early stage of disease with relatively preserved central visual function while patch and atrophy represent advanced disease with moderate to severe loss of vision.

4.1. Fundus autofluorescence abnormalities

Murakami et al. classified FAF patterns of RP patients including one Usher patient into patterns of ring, central hyperautofluorescence and absence of both. They hypothesized different patterns could be a result of different pathogenesis or different disease stages (Murakami et al., 2008). We have also found patterns of ring and central hyperautofluorescence (patch), however no patients had absence of both and we also had a group of patients with central hypoautofluorescence which they have not described. Difference in our findings could be a result of different stages of the disease or differences between Usher syndrome and nonsyndromic RP. In a few cases it was difficult to distinguish between ring and patch on FAF (examples in Fig. 4E). It is possible that those cases represent intermediary stages between ring and patch pattern, which could be confirmed with longitudinal FAF imaging. While it is known that abnormal FAF can be seen in patients with retinitis pigmentosa, the location of fluorophores in the retina contributing to hyperautofluorescence is not clear. Recently it has been proposed that photoreceptor cells could be a major source of autofluorescence in pathological states (Sparrow et al., 2010). OCT findings in the ring and patch area suggest absence of outer segments in those areas. We propose that photoreceptor inner segments or cell bodies could be the location of abnormal bisretinoid accumulation, possibly contributing to photoreceptor apoptosis (Cottet & Schorderet, 2009; Maeda et al., 2008).

4.2. OCT findings

The hyper-reflective band representing ELM appeared to be intact across the foveal area in all eyes with rings or patches and absent in eyes with central hypoautofluorescence. ELM length correlated closely with outer ring border and patch border, contributing to the idea that patch is a stage following ring. Central remains of ISe were seen in all patients with rings and showed good spatial correlation with the area of normal autofluorescence inside the ring. In patients with patches, ISe was either absent or had radius shorter than 0.5 mm (foveal radius). Spatial correlation between AF and OCT structures was not always exact, i.e. inner ring border was measured in average 0.1 mm closer to the fovea than ISe loss. An explanation for this could be measurement error, especially in recognizing the exact location of inner ring border due to rising signal of autofluorescence from the foveal center towards the periphery or due to presence of CME (Fig. 8C).

4.3. FAF and OCT in relation to visual function

Hyperautofluorescent ring was associated with relatively preserved central visual function, which is in agreement with previous studies (Popovic, Jarc-Vidmar, & Hawlina, 2005; Robson et al., 2003, 2004, 2006). Nevertheless some loss of central vision was observed in majority of patients even at this stage. Visual acuity and color vision were lower in patients with ring radius smaller than 3° and the dimmest (II/1) Goldmann target was often not detected by those patients (see Section 3.4). Patients with ISe radius smaller than radius of fovea were most affected (Fig. 7). Similarly, decrease in VA associated with ring constriction was described in rings smaller than 0.68 mm (2.5°) in radius (Aizawa et al., 2010). These findings could be explained by deterioration of retinal structure inside the rings that has been described in literature, such as shortening of outer segments and ONL thinning in areas of preserved ISe (Hood et al., 2011) and reduced cone numbers inside the rings (Greenstein et al. IOVS, 2012; 53: ARVO E-Abstract 4577).

Microperimetry and fine matrix mapping studies have shown strong spatial correspondence between sensitivity losses and the internal edge of the ring (Lenassi et al., 2012; Robson et al., 2004, 2012). They have shown that sensitivity is well preserved inside the ring of hyperautofluorescence and decreases with eccentricity. We have also found good sensitivity inside the ring and decreased sensitivity outside the ring using Goldmann perimetry (stimulus II/1 was detected only inside while II/4 and V/4 were detected outside the ring in most patients). Large Goldmann target with high intensity (V/4) was used to determine how far from the ring any light stimulus can still be detected. Our results suggest that although abnormal, there usually is some cone function up to

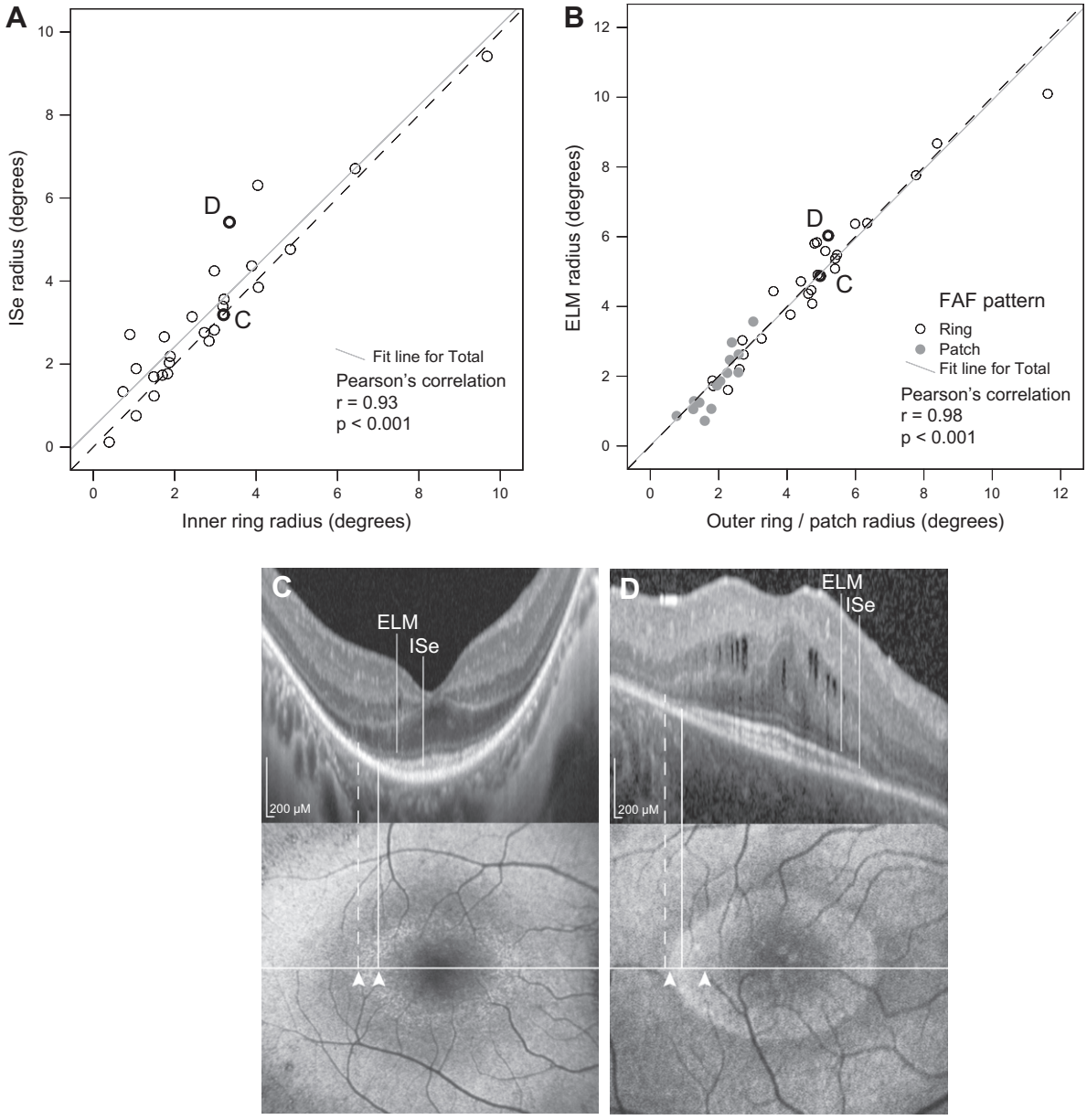

Fig. 8. (A) Correlation between horizontal span of ISe and radius of inner ring border. (B) Correlation between horizontal span of ELM and radius outer ring border. Dashed line on graph represent a situation where radius of measured structure on OCT equals radius of measured ring or patch border. (C and D) Two examples of spatial correlations between FAF and OCT structures (cases are also marked on the graphs with letters C and D). Dashed and full white lines represent point of ELM and ISe disruption, respectively. Arrowheads represent outer and inner border of the hyperautofluorescent ring. ISe = inner segment ellipsoid, ELM = external limiting membrane.

about 7° outside from the ring. Interestingly, histological analysis of RP retinas have shown that when all rods and most of the cones are lost, the macula usually retains a monolayer of cone somata with very short or absent outer segments (Milam, Li, & Fariss, 1998), which might explain this residual cone function.

Hyperautofluorescent foveal patch was seen in patients with several decades of disease duration and was associated with significant loss of central visual function and ONL thinning (Table 2), reflecting loss of photoreceptor cells in the fovea. Visual acuity was relatively preserved only in patients with central remains of ISe, which might represent a transition from ring to patch. Abnormal central hypoautofluorescence (foveal atrophy) was seen in 5 eyes and was associated with the most severe loss of retinal structure and function. Limitation of the current study is that scotopic macular function was not examined as all examinations were performed under photopic conditions and therefore only function of cones could be evaluated.

4.4. Disease progression

Serial FAF imaging of rings in patients with short disease duration and the presence of central FAF abnormalities in cases with long-standing disease suggest that rings constrict with time and may eventually be replaced by central FAF abnormalities (hyperautofluorescent patch and atrophy) associated with visual acuity loss. This is in keeping with published data that demonstrated progression from a ring to central hyperautofluorescence in a few individuals (Robson et al., 2011; Wakabayashi et al., 2010). Additonally, we have observed progression from central hyperautofluorescence (patch) to central hypoautofluorescence (atrophy) in three patients (example in Fig. 3C).

Average rate of disease progression in the macula was estimated by measuring ring constriction and was 4% per year. This is in good agreement with two previously published papers. Lima et al. reported rates of inner border constriction for two patients

Table 2
Differences in retinal structure and function between patients with large ring, small ring, patch or atrophy. Patients with CME, cataract, macular traction or posterior capsular opacification are excluded. Values which are significantly different between each other are marked in bold (ANOVA, LSD post hoc test, $p < 0.05$). *y* = Years, ELM = external limiting membrane, ISe = inner segment ellipsoid, ONL = outer nuclear layer, VA = visual acuity, N/A = not applicable.

FAF pattern	Large ring ($r \geqslant 3°$)	Small ring ($r < 3°$)	Patch	Atrophy	Pearson's correlation (r, p)
N	8	12	18	5	
Age (average, range)	31y (7–58)	37y (23–54)	50y (32–69)	51y (29–69)	0.5, <0.001
Disease duration (average, range)	13y (2–26)	**22y** (4–33)	**37y** (9–54)	44y (25–60)	0.7, <0.001
Retinal structure (average, range)					
Outer ring border/patch radius	**6**° (4–12)	**4**° (2–8)	**2**° (1–3)	N/A	−0.8, <0.001
ELM radius	**6**° (4–10)	**4**° (2–8)	**2**° (1–4)	N/A	−0.8, <0.001
Inner ring border radius	**5**° (3–10)	**2**° (1–3)	NA	N/A	−0.7, <0.001
ISe radius	**5**° (3–9)	**2**° (1–4)	**1**° (0–2)	N/A	−0.8, <0.001
ONL thickness in fovea	114 μm (93–129)	**108 μm** (63–182)	**56 μm** (36–88)	N/A	−0.8, <0.001
Retinal function (average, range)					
VA	0.9 (0.5–1.0)	**0.7** (0.3–1.0)	**0.2** (0.001–0.6)	0.04 (0–0.15)	−0.8, <0.001
Number of recognized Ishihara tables	**12** (1–15)	**6** (0–13)	**1** (0–6)	0 (0–1)	−0.8, <0.001
II/1 visual field radius	**3**° (1–7)	**1**° (0–2)	N/A	N/A	−0.8, <0.001
II/4 visual field radius	**14**° (6–25)	**7**° (2–13)	**3**° (0–9)	3° (0–6)	−0.7, <0.001
Average sensitivity in central 8°	**13 dB** (7–19)	**6 dB** (1–13)	**1 dB** (0–7)	0 dB (0–1)	−0.8, <0.001

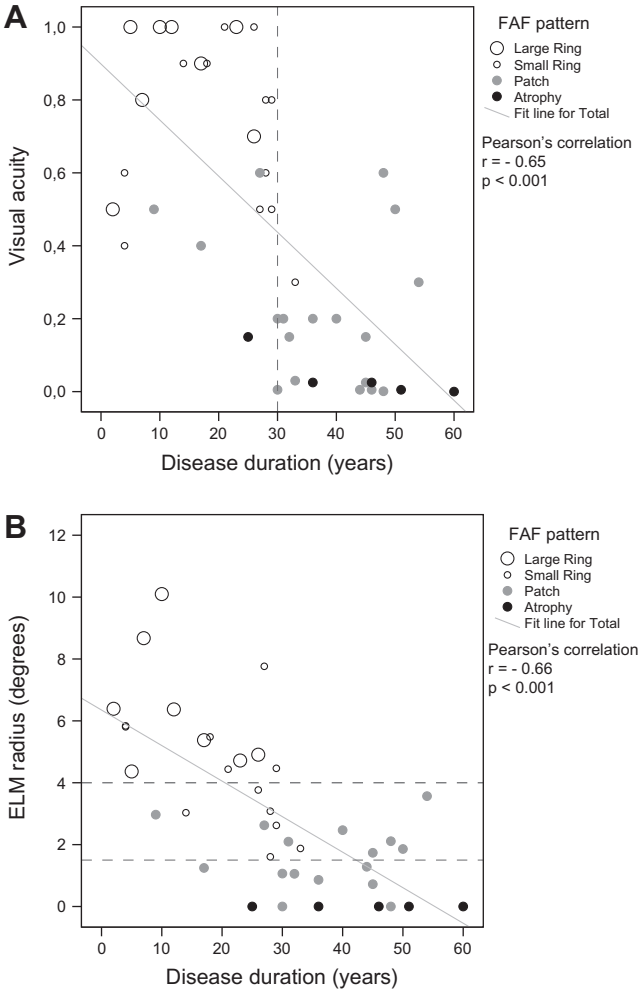

Fig. 9. (A) Visual function (A) and retinal structure (B) in association with disease duration. Different FAF patterns are marked (see legend). (A) Significant loss of visual acuity was seen after 30 years of disease, associated with patch or atrophy on fundus autofluorescence. (B) ELM was shorter in patients with longer disease duration. At ELM radius between 1.5° and 4°, rings or patch could be observed. FAF = fundus autofluorescence, ELM = external limiting membrane.

with recessive RP. Average rate of constriction was calculated from their data to be 4% per year (Lima et al., 2012). Robson et al. reported inner border constriction in 6/12 Usher patients. Taken all 12 patients together, their average rate of constriction was calculated at 5% per year (Robson et al., 2011). Reported rates of visual field constriction are somewhat higher (6–9%) (Fishman et al., 2007; Iannaccone et al., 2004; Sandberg et al., 2008).

4.5. Disease expression in different types of Usher syndrome

The existence of different clinical subtypes of Usher syndrome based on hearing loss have been known for a long time, however possible differences in retinal phenotype have been controversial. Apart from earlier disease onset in USH1 we have not found any other differences in disease expression. We found the same basic FAF patterns in USH1 and USH2 patients as well as in all three the most commonly affected genes (*USH2A*, *MYO7A* and *PCDH15*). Similarly, Jacobson et al. have not found any differences when analyzing OCT of *MYO7A*, *PCDH15*, *USH2A* and *GPR98* patients (Jacobson et al., 2008). When separately analyzing patients with short and long-standing disease, USH1 patients did not have significantly higher frequency of foveal lesions than USH2. There was also no significant difference between age and disease duration between USH1 and USH2 patients with legal blindness. We cannot exclude a possibility that specific genes or mutations produce variations of disease expression such as some of the features seen in our sibling pairs; however this should be confirmed in large groups of genotype specific patients with the same disease stage.

4.6. Conclusion

The present study provides an opportunity to increase understanding of retinal disease in Usher syndrome. Central vision remained relatively preserved in most Usher patients for up to three decades after onset of nyctalopia. After three decades the fovea was usually involved, reflected by loss of central visual function. Hyperautofluorescent foveal patch was the hallmark of this stage. Understanding the natural history of retinal disease in Usher syndrome will be important in the prospect of clinical trials.

Contributors

Ana Fakin: Microperimetry, OCT, Goldmann, morphological and statistical analysis, concept and article preparation.

Martina Jarc-Vidmar: Performed ophthalmologic examination, morphological analysis and article preparation.

Damjan Glavač: Contributed to genetic analysis and article preparation.

Crystel Bonnet: Performed genetic sequencing of Usher genes.

Christine Petit: Contributed to genetic analysis and article preparation.

Marko Hawlina: Performed ophthalmologic examinations, morphological analysis, concept and article preparation.

All authors have approved the final article.

Financial support

Slovenian research agency (ARRS P3-0333, Treatrush (HEALTH-F2-2010-242013), European Collaborative project, LHW-Stiftung, Fondation R&G Strittmatter, FAUN Stiftung (Suchert Foundation). No involvement in study design, collection, analysis and interpretation of data, writing of the report or in the decision to submit the article for publication.

Acknowledgment

Authors wish to thank the staff of the Eye Hospital, University Medical Centre Ljubljana for help with imaging, visual field examinations and acquiring the blood samples.

References

Aizawa, S., Mitamura, Y., Hagiwara, A., Sugawara, T., & Yamamoto, S. (2010). Changes of fundus autofluorescence, photoreceptor inner and outer segment junction line, and visual function in patients with retinitis pigmentosa. *Clinical & Experimental Ophthalmology, 38*(6), 597–604.

Bonnet, C., & El-Amraoui, A. (2011). Usher syndrome (sensorineural deafness and retinitis pigmentosa): Pathogenesis, molecular diagnosis and therapeutic approaches. *Current Opinion in Neurology, 25*(1), 42–49.

Boughman, J. A., Vernon, M., & Shaver, K. A. (1983). Usher syndrome: Definition and estimate of prevalence from two high-risk populations. *Journal of Chronic Diseases, 36*(8), 595–603.

Cohen, M., Bitner-Glindzicz, M., & Luxon, L. (2007). The changing face of Usher syndrome: Clinical implications. *International Journal of Audiology, 46*(2), 82–93.

Cottet, S., & Schorderet, D. F. (2009). Mechanisms of apoptosis in retinitis pigmentosa. *Current Molecular Medicine, 9*(3), 375–383.

Edwards, A., Fishman, G. A., Anderson, R. J., Grover, S., & Derlacki, D. J. (1998). Visual acuity and visual field impairment in Usher syndrome. *Archives of Ophthalmology, 116*(2), 165–168.

Fishman, G. A., Anderson, R. J., Lam, B. L., & Derlacki, D. J. (1995). Prevalence of foveal lesions in type 1 and type 2 Usher's syndrome. *Archives of Ophthalmology, 113*(6), 770–773.

Fishman, G. A., Bozbeyoglu, S., Massof, R. W., & Kimberling, W. (2007). Natural course of visual field loss in patients with Type 2 Usher syndrome. *Retina, 27*(5), 601–608.

Hood, D. C., Lazow, M. A., Locke, K. G., Greenstein, V. C., & Birch, D. G. (2011). The transition zone between healthy and diseased retina in patients with retinitis pigmentosa. *Investigative Ophthalmology & Visual Science, 52*(1), 101–108.

Hope, C. I., Bundey, S., Proops, D., & Fielder, A. R. (1997). Usher syndrome in the city of Birmingham—Prevalence and clinical classification. *British Journal of Ophthalmology, 81*(1), 46–53.

Iannaccone, A., Kritchevsky, S. B., Ciccarelli, M. L., Tedesco, S. A., Macaluso, C., Kimberling, W. J., & Somes, G. W. (2004). Kinetics of visual field loss in Usher syndrome Type II. *Investigative Ophthalmology & Visual Science, 45*(3), 784–792.

Jacobson, S. G., Cideciyan, A. V., Aleman, T. S., Sumaroka, A., Roman, A. J., Gardner, L. M., Prosser, H. M., Mishra, M., Bech-Hansen, N. T., Herrera, W., Schwartz, S. B., Liu, X. Z., Kimberling, W. J., Steel, K. P., & Williams, D. S. (2008). Usher syndromes due to MYO7A, PCDH15, USH2A or GPR98 mutations share retinal disease mechanism. *Human Molecular Genetics, 17*(15), 2405–2415.

Kimberling, W. J., Moller, C. G., Davenport, S. L., Lund, G., Grissom, T. J., Priluck, I., White, V., Weston, M. D., Biscone-Halterman, K., & Brookhouser, P. E. (1989). Usher syndrome: Clinical findings and gene localization studies. *Laryngoscope, 99*(1), 66–72.

Lefevre, G., Michel, V., Weil, D., Lepelletier, L., Bizard, E., Wolfrum, U., Hardelin, J. P., & Petit, C. (2008). A core cochlear phenotype in USH1 mouse mutants implicates fibrous links of the hair bundle in its cohesion, orientation and differential growth. *Development, 135*(8), 1427–1437.

Lenassi, E., Troeger, E., Wilke, R., & Hawlina, M. (2012). Correlation between macular morphology and sensitivity in patients with retinitis pigmentosa and hyperautofluorescent ring. *Investigative Ophthalmology & Visual Science, 53*(1), 47–52.

Lima, L. H., Burke, T., Greenstein, V. C., Chou, C. L., Cella, W., Yannuzzi, L. A., et al. (2012). Progressive constriction of the hyperautofluorescent ring in retinitis pigmentosa. *American Journal of Ophthalmology, 153*(4), 718–727, 727, e711–712.

Maeda, A., Maeda, T., Golczak, M., & Palczewski, K. (2008). Retinopathy in mice induced by disrupted all-trans-retinal clearance. *Journal of Biological Chemistry, 283*(39), 26684–26693.

Maerker, T., van Wijk, E., Overlack, N., Kersten, F. F., McGee, J., Goldmann, T., Sehn, E., Roepman, R., Walsh, E. J., Kremer, H., & Wolfrum, U. (2008). A novel Usher protein network at the periciliary reloading point between molecular transport machineries in vertebrate photoreceptor cells. *Human Molecular Genetics, 17*(1), 71–86.

Milam, A. H., Li, Z. Y., & Fariss, R. N. (1998). Histopathology of the human retina in retinitis pigmentosa. *Progress in Retinal and Eye Research, 17*(2), 175–205.

Millan, J. M., Aller, E., Jaijo, T., Blanco-Kelly, F., Gimenez-Pardo, A., & Ayuso, C. (2011). An update on the genetics of usher syndrome. *Journal of Ophthalmology, 2011*, 417217.

Mitamura, Y., Mitamura-Aizawa, S., Nagasawa, T., Katome, T., Eguchi, H., & Naito, T. (2012). Diagnostic imaging in patients with retinitis pigmentosa. *Journal of Medical Investigation, 59*(1–2), 1–11.

Murakami, T., Akimoto, M., Ooto, S., Suzuki, T., Ikeda, H., Kawagoe, N., Takahashi, M., & Yoshimura, N. (2008). Association between abnormal autofluorescence and photoreceptor disorganization in retinitis pigmentosa. *American Journal of Ophthalmology, 145*(4), 687–694.

Piazza, L., Fishman, G. A., Farber, M., Derlacki, D., & Anderson, R. J. (1986). Visual acuity loss in patients with Usher's syndrome. *Archives of Ophthalmology, 104*(9), 1336–1339.

Popovic, P., Jarc-Vidmar, M., & Hawlina, M. (2005). Abnormal fundus autofluorescence in relation to retinal function in patients with retinitis pigmentosa. *Graefes Archive for Clinical and Experimental Ophthalmology, 243*(10), 1018–1027.

Robson, A. G., Egan, C., Holder, G. E., Bird, A. C., & Fitzke, F. W. (2003). Comparing rod and cone function with fundus autofluorescence images in retinitis pigmentosa. *Advances in Experimental Medicine and Biology, 533*, 41–47.

Robson, A. G., Egan, C. A., Luong, V. A., Bird, A. C., Holder, G. E., & Fitzke, F. W. (2004). Comparison of fundus autofluorescence with photopic and scotopic fine-matrix mapping in patients with retinitis pigmentosa and normal visual acuity. *Investigative Ophthalmology & Visual Science, 45*(11), 4119–4125.

Robson, A. G., Lenassi, E., Saihan, Z., Luong, V., Fitzke, F., Holder, G. E., et al. (2012). Comparison of fundus autofluorescence with photopic and scotopic fine matrix mapping in patients with retinitis pigmentosa: 4- to 8-year follow-up. *Investigative Ophthalmology & Visual Science*.

Robson, A. G., Saihan, Z., Jenkins, S. A., Fitzke, F. W., Bird, A. C., Webster, A. R., & Holder, G. E. (2006). Functional characterisation and serial imaging of abnormal fundus autofluorescence in patients with retinitis pigmentosa and normal visual acuity. *British Journal of Ophthalmology, 90*(4), 472–479.

Robson, A. G., Tufail, A., Fitzke, F., Bird, A. C., Moore, A. T., Holder, G. E., & Webster, A. R. (2011). Serial imaging and structure-function correlates of high-density rings of fundus autofluorescence in retinitis pigmentosa. *Retina, 31*(8), 1670–1679.

Saihan, Z., Webster, A. R., Luxon, L., & Bitner-Glindzicz, M. (2009). Update on Usher syndrome. *Current Opinion in Neurology, 22*(1), 19–27.

Sandberg, M. A., Rosner, B., Weigel-DiFranco, C., McGee, T. L., Dryja, T. P., & Berson, E. L. (2008). Disease course in patients with autosomal recessive retinitis pigmentosa due to the USH2A gene. *Investigative Ophthalmology & Visual Science, 49*(12), 5532–5539.

Seeliger, M., Pfister, M., Gendo, K., Paasch, S., Apfelstedt-Sylla, E., Plinkert, P., Zenner, H. P., & Zrenner, E. (1999). Comparative study of visual, auditory, and olfactory function in Usher syndrome. *Graefes Archive for Clinical and Experimental Ophthalmology, 237*(4), 301–307.

Sparrow, J. R., Yoon, K. D., Wu, Y., & Yamamoto, K. (2010). Interpretations of fundus autofluorescence from studies of the bisretinoids of the retina. *Investigative Ophthalmology & Visual Science, 51*(9), 4351–4357.

Tsilou, E. T., Rubin, B. I., Caruso, R. C., Reed, G. F., Pikus, A., Hejtmancik, J. F., Iwata, F., Redman, J. B., & Kaiser-Kupfer, M. I. (2002). Usher syndrome clinical types I and II: Could ocular symptoms and signs differentiate between the two types? *Acta Ophthalmologica Scandinavica, 80*(2), 196–201.

van Soest, S., Westerveld, A., de Jong, P. T., Bleeker-Wagemakers, E. M., & Bergen, A. A. (1999). Retinitis pigmentosa: Defined from a molecular point of view. *Survey of Ophthalmology, 43*(4), 321–334.

Wakabayashi, T., Sawa, M., Gomi, F., & Tsujikawa, M. (2010). Correlation of fundus autofluorescence with photoreceptor morphology and functional changes in eyes with retinitis pigmentosa. *Acta Ophthalmologica, 88*(5), e177–e183.

Williams, D. S. (2008). Usher syndrome: Animal models, retinal function of Usher proteins, and prospects for gene therapy. *Vision Research, 48*(3), 433–441.